

A Deep Search for a Strong Diffuse Interstellar Band in the Circumgalactic Medium

CHIH-YUAN CHANG^{1,2} AND TING-WEN LAN^{3,1,2}

¹*Department of Physics, National Taiwan University, No. 1, Sec. 4, Roosevelt Rd., Taipei 10617, Taiwan*

²*Institute of Astronomy and Astrophysics, Academia Sinica, No. 1, Sec. 4, Roosevelt Rd., Taipei 10617, Taiwan*

³*Graduate Institute of Astrophysics, National Taiwan University, No. 1, Sec. 4, Roosevelt Rd., Taipei 10617, Taiwan*

ABSTRACT

We investigate the absorption signals of a strong diffuse interstellar band, DIB λ 4430, in the circumgalactic medium (CGM) traced by MgII absorption lines. To this end, we make use of approximately 60,000 MgII absorption line spectra within $0.4 < z < 1.0$ compiled from the Sloan Digital Sky Surveys and obtain composite spectra with uncertainties for absorption line measurements being a few mÅ. By using MgII absorption strength and dust reddening relation from the literature, we measure the DIB λ 4430 absorption strength as a function of $E(B - V)$ in the CGM, and compare the Milky Way DIB λ 4430 - $E(B - V)$ relation extrapolated down to the CGM $E(B - V)$ region. Our results show no detectable signals of DIB λ 4430 across the entire $E(B - V)$ range in the CGM traced by MgII absorption lines. This lack of detection of DIB λ 4430 in the CGM is inconsistent with the Milky Way signals by $\sim 5\sigma$, indicating that the factors associated with different environments affect the abundance of the DIB λ 4430 carrier.

Keywords: Diffuse interstellar bands (379), Circumgalactic medium (1879), and Intergalactic dust clouds (810)

1. INTRODUCTION

Diffuse interstellar bands (DIBs) are weak absorption features that have been detected ubiquitously in the Milky Way and other galaxies (e.g., Jenniskens & Désert 1994; Hobbs et al. 2008, 2009; Cordiner et al. 2011; Baron et al. 2015; Lan et al. 2015). The first discovery of DIBs dates back to 1919 (Heger 1922) with the detection of two DIBs (λ 5780 and λ 5797) in the stellar spectra within our Milky Way, which were later found to be interstellar in origin (Merrill 1934; Merrill & Wilson 1938). In total, over 500 DIBs have been found (e.g., Hobbs et al. 2008, 2009). It is speculated that the sources of these absorption features are large organic molecules such as polycyclic aromatic hydrocarbons (PAHs) (e.g., Crawford et al. 1985; Léger & D’Hendecourt 1985), fullerenes (e.g., Léger et al. 1988), or fulleranes (e.g., Webster 1993). In 2015, laboratory studies confirmed C_{60}^+ to be the carrier of two DIBs, λ 9632 and λ 9577 (Campbell et al. 2015), and further studies (e.g. Campbell et al. 2016; Cordiner et al. 2017; Campbell & Maier 2018; Cordiner et al. 2019) have identified three more DIBs as arising from C_{60}^+ transitions within the interstellar medium (Linnartz et al. 2020). These results

demonstrate that large complex molecules similar to C_{60} are possible carriers for other DIBs.

To assist the identification of DIB carriers, one can detect and characterize the properties of DIBs in different environments (e.g., Jenniskens & Désert 1994; Galazutdinov et al. 2000; van Loon et al. 2013; Welty 2014; Baron et al. 2015; Lan et al. 2015; Elyajouri et al. 2017; Schultheis et al. 2023). Previous studies have mostly focused on probing DIBs in the relatively gas-rich and dusty environments in our Milky Way, where DIB absorptions have been found to be stronger (e.g. Baron et al. 2015; Lan et al. 2015). There are also explorations of DIBs in the interstellar medium (ISM) of other galaxies (e.g., Cordiner 2014). For example, DIBs have been detected in Large and Small Magellanic clouds (e.g., Welty et al. 2006; Bailey et al. 2015) and local starburst galaxies (e.g., Heckman & Lehnert 2000; Welty et al. 2014). In addition, the abundances of DIBs have been investigated in quasar absorption line systems with high neutral hydrogen column densities (DLAs, damped Ly α system, York et al. 2006; Lawton et al. 2008) and with high metal column densities (CaII) (Ellison et al. 2008). However, due to their weak absorption strengths, the content of DIBs in low-density environments, such as in the circumgalactic medium (CGM, Tumlinson et al. 2017), has not been explored.

In this work, we make use of the large spectroscopic dataset provided by the Sloan Digital Sky Surveys

(SDSS) (York et al. 2000) and perform a deep search for one of the strongest DIBs, DIB λ 4430 (e.g., Walker 1963; Snow 2002; Snow et al. 2002), in the CGM. We use MgII absorption lines detected in quasar spectra as a tracer of the cool CGM ($T \sim 10^4$ K) (e.g., Lan et al. 2018; Lan 2020; Anand et al. 2021) and obtain high signal-to-noise (S/N) composite spectra by combining tens of thousands of individual absorption line spectra. This allows us to probe weak DIBs absorbing $\sim 0.1\%$ of the continuum.

The structure of the paper is as follows. In Section 2, we detail the data analysis process, including the data and the methodology of obtaining the composite spectra. We summarize the results and discuss the implications of our findings in Section 3. We conclude this work in Section 4. Throughout the paper, we use vacuum wavelength.

2. DATA ANALYSIS

2.1. Composite spectra for DIB λ 4430

To probe DIB λ 4430 in the CGM traced by MgII absorption lines, we use a large MgII absorption catalog¹ compiled by Anand et al. (2021) from the Sloan Digital Sky Survey DR16 dataset (Lyke et al. 2020). In total, the catalog contains $\sim 160,000$ MgII absorbers with redshifts ranging from 0.36 to 2.28 (Anand et al. 2021). In order to detect DIB λ 4430 in the SDSS optical spectra, we select MgII absorbers with redshifts between $0.4 < z < 1.0$. This yields 60,650 MgII absorbers with a median redshift of ~ 0.7 .

To further combine individual absorption spectra, we follow a similar procedure as Zhu et al. (2014). We first estimate the intrinsic spectral energy distributions (SEDs) of the quasars by using a set of quasar eigen-spectra obtained by applying non-negative matrix factorization technique (implemented by Zhu (2016)) to the SDSS quasar spectra from Zhu & Ménard (2013). The original spectra are then normalized by the NMF-reconstructed quasar SEDs. We further apply a median filter with 71 pixels to the normalized spectrum to obtain a median continuum for capturing small-scale fluctuation with the pixels between 4420 and 4440 Å being masked. The final normalized spectrum is the ratio between the normalized spectrum and the median continuum. All the normalized spectra are shifted into the rest-frame of the MgII absorbers and projected onto a common wavelength grid with the SDSS spectral resolution. We combine individual spectra with a median estimator to avoid effects of outliers in the spectra. We note that this method has been used to detect weak spectral features in previous works (e.g., Zhu & Ménard 2013; Zhu et al. 2014; Lan & Fukugita 2017; Lan et al. 2018; Ng et al. 2025). Finally, we obtain high signal-to-noise

composite spectra as a function of the rest equivalent widths of MgII absorption lines ($W_0^{\lambda 2796}$). Table 1 summarizes the number of individual spectra used in the composite spectra.

Table 1. Number of spectra used in each composite spectrum as a function of $W_0^{\lambda 2796}$

$W_0^{\lambda 2796}$ [Å]	Number of Spectra
$0.40 < W_0^{\lambda 2796} < 0.66$	7641
$0.66 < W_0^{\lambda 2796} < 1.09$	18453
$1.09 < W_0^{\lambda 2796} < 1.82$	22640
$1.82 < W_0^{\lambda 2796} < 3.07$	10959
$3.07 < W_0^{\lambda 2796}$	957

To measure possible weak DIB λ 4430 signals from the composite spectra, we fit a Gaussian profile with a fixed line width $\sigma = 6.9$ Å and a fixed central wavelength at 4429.9 Å, the best-fit parameters of Milky Way sightlines from Lan et al. (2015). The uncertainty of absorption strength is estimated via bootstrapping the sample 500 times.

2.2. Dust reddening of MgII absorbers

In order to compare the DIB λ 4430 signals in the CGM traced by MgII absorbers and the DIB λ 4430 signals observed in the Milky Way with a given dust content along the lines of sight, we use the $W_0^{\lambda 2796}$ and dust reddening $E(B-V)$ based on Ménard & Fukugita (2012) and Ménard et al. (2008) with

$$E(B-V)_{obs} \simeq \frac{E(g-i)_{obs}}{1.55} \simeq \frac{0.017}{1.55} \times \left(\frac{W_0^{\lambda 2796}}{1\text{Å}} \right)^{1.6}, \quad (1)$$

$$E(B-V)_{rest} = E(B-V)_{obs} \times (1+z)^{-1.2} \quad (2)$$

where $E(g-i)_{obs}$ is the dust reddening with SDSS g and i bands in observed frame, $E(B-V)_{obs}$ is the estimated reddening with SMC like extinction curve (York et al. 2006; Ménard & Fukugita 2012), and $E(B-V)_{rest}$ is the reddening in the rest-frame. The above parameter values are adopted from Ménard & Fukugita (2012) and Ménard et al. (2008) based on the color excess signals induced by MgII absorbers.

For the DIB λ 4430 signals in the Milky Way, we use the DIB λ 4430 absorption strength based on the relation observed in the Milky Way from Lan et al. (2015):

$$W_0^{\lambda 4430}(E(B-V)) = 1.22(E(B-V)_{rest})^{0.89} \text{Å}. \quad (3)$$

We note that the average $E(B-V)$ value for MgII absorbers with $W_0^{\lambda 2796} \sim 1$ Å is ~ 0.005 mag, which is lower than a typical Milky Way sightline. Therefore, the expected MW DIB signals are extrapolated values based on the best-fit relation from $E(B-V) > 0.04$ mag sightlines (Lan et al. 2015).

¹ <https://wwwmpa.mpa-garching.mpg.de/SDSS/MgII/>

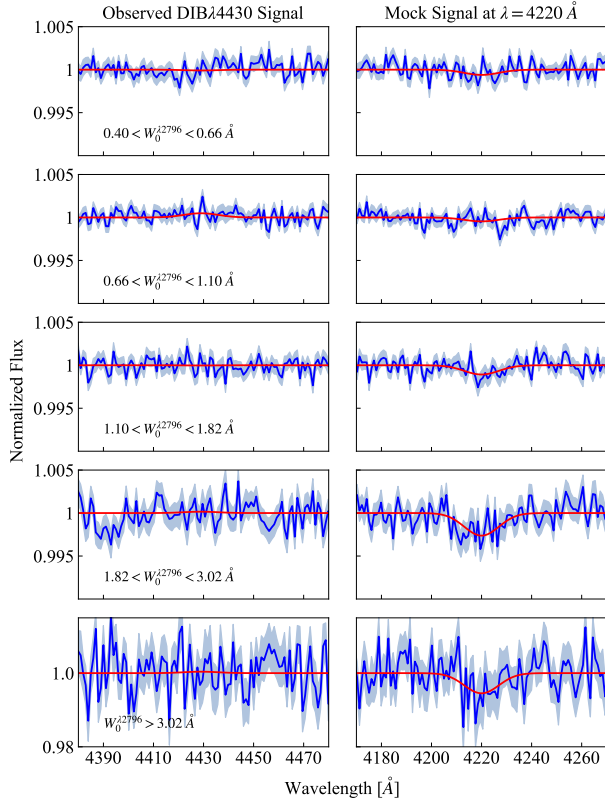


Figure 1. Composite spectra as a function of $W_0^{\lambda 2796}$. The blue solid lines show the composite spectra with bootstrap uncertainties indicated by the shaded bands. The red solid lines are the best-fit absorption profiles. *Left:* observed spectral regions around DIB $\lambda 4430$. *Right:* spectral regions around 4220 Å with synthetic absorption signals recovered.

Combining $E(B-V)$ in MgII absorbers and the correlation between DIB $\lambda 4430$ and $E(B-V)$ in our Milky Way, we compare DIB signals in the CGM and the expected signals in the Milky Way with the same $E(B-V)$ value.

3. RESULTS AND DISCUSSION

The composite spectra are shown in Figure 1. The left panels show the spectral regions around DIB $\lambda 4430$. The solid lines are the composite spectra with bootstrapping uncertainties indicated by the shaded regions. The red solid lines show the best-fit profiles for measuring the possible absorption strengths of DIB $\lambda 4430$. The rest equivalent width of DIB $\lambda 4430$ as a function of MgII absorption and $E(B-V)$ are shown in Figure 2. We do not detect any DIB $\lambda 4430$ absorption throughout the range of $E(B-V)$ traced by MgII absorbers. To quantify the overall trend, we fit our measured $W_0^{\lambda 4430}$ as a function of $E(B-V)$ with

$$W_0^{\lambda 4430} = A \times E(B-V)^{0.89}, \quad (4)$$

where the power index 0.89 is the expected value based on the Milky Way relation (Eq. 3). The best-fit value of A is -0.16 ± 0.23 being consistent with no detection. This non-detection result deviates from the expected signals based on the $W_0^{\lambda 4430} - E(B-V)$ relation (black line in Figure 2) from the Milky Way sightlines (Lan et al. 2015).

To further test the results, we insert mock DIB absorption lines at 4220 Å in the rest frame of MgII absorbers into the original SDSS quasar spectra with the strengths following the $W_0^{\lambda 4430} - E(B-V)$ relation in the Milky Way (Eq. 3). This spectral region is chosen for its lack of absorption features. We run the same pipeline, which includes NMF normalization and median filter, to obtain the median composite spectra. The right panels of Figure 1 show the composite spectra around 4220 Å. The red solid lines show the best-fit absorption profiles, recovering the input signals. The blue data points in Figure 2 are the recovered signals, which are consistent with input signals (black solid line). We also fit the mock signals with Eq. 4 and obtain the best-fit value of A_{mock} being 1.39 ± 0.22 , which is consistent with the input relationship (Eq. 3). Based on the non-detection of DIB $\lambda 4430$ and the corresponding uncertainty, our result shows that the $W_0^{\lambda 4430} - E(B-V)$ relation in the CGM traced by MgII absorbers deviates from the Milky Way relationship by 5.3σ .

In Figure 2, we also overplot the 3σ upper limits of DIB $\lambda 4430$ absorption strengths in damped Lyman alpha systems (DLAs) from Lawton et al. (2008) (purple data points). The authors searched for DIBs in seven DLAs and detected DIBs in only one system having the highest reddening and metallicity. They also reached to a similar conclusion that the DIB- $E(B-V)$ relation in the DLAs is deviated from the Milky Way relation. This trend is also observed in the Large and Small Magellanic Clouds, showing weaker DIB absorption lines than values based on Milky Way DIB - dust/gas relation (Welty et al. 2006).

Our results indicate that with the same $E(B-V)$ value, the abundances of the DIB $\lambda 4430$ carrier in the ISM and in the CGM are significantly different, indicating that factors associated with different environments play a key role in regulating the abundance of the DIB $\lambda 4430$ carrier. Here we discuss possible factors for the different strengths of DIB $\lambda 4430$ in the MW and in MgII absorbers:

- **Production of the DIB carrier:** One possibility is that a certain environment is required to form the DIB $\lambda 4430$ carrier; the Milky Way has such an environment while the circumgalactic gas traced by MgII absorbers and galaxies producing the gas do not have such an environment. This might possibly link to the 2175Å bump in the extinction curve. Both the Milky Way (e.g., Fitzpatrick & Massa 2007) and the

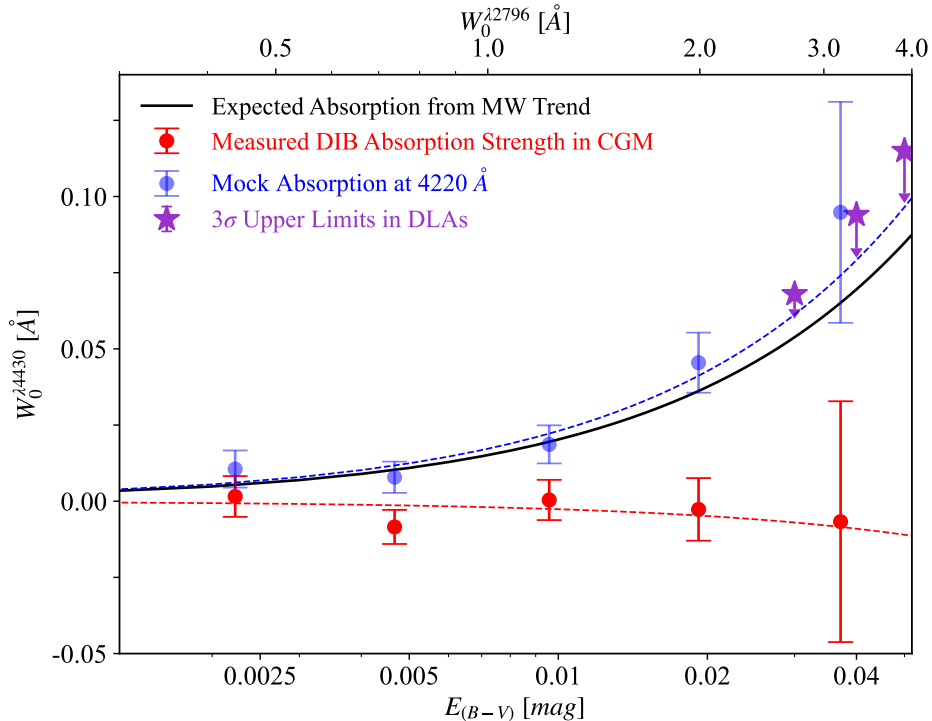


Figure 2. DIB λ 4430 absorption strengths as a function of $W_0^{\lambda 2796}$ and $E(B - V)$. The red data points show the measured absorption strengths at DIB λ 4430 and the blue data points show the measured absorption strengths for the synthetic absorption profiles at 4220 Å. The corresponding color dashed lines show the best-fit power laws. The black solid line shows the Milky Way DIB λ 4430 - $E(B - V)$ relation which is recovered from the synthetic signals (blue line). The purple stars show 3σ upper limits derived from damped Lyman-alpha systems (Lawton et al. 2008).

DLA with DIB λ 4430 detected (Junkkarinen et al. 2004) have the 2175Å bump in their extinction curves, while SMC and MgII absorbers (York et al. 2006; Ménard & Fukugita 2012) have similar extinction curves without the bump and weaker DIB absorption strength. We note that while the correlation between 2175Å bump and DIB λ 4430 is still under debate (e.g., Xiang et al. 2017; Cox et al. 2007; Iglesias-Groth 2007), if the correlation is further confirmed, it indicates that the environments under certain conditions can grow materials being responsible for 2175Å extinction bump and DIB λ 4430.

- **Destruction of the DIB carrier:** Given that MgII absorbers trace the circumgalactic gas clouds with part of the materials expected to be ejected from galaxies through feedback mechanisms (e.g., Bordoloi et al. 2011; Lan et al. 2018), it is possible that with the energy from stellar explosions, the carrier of DIB λ 4430 is ionized and/or destroyed during the transportation process, similar to the dust destruction due to supernovae (e.g., Priestley et al. 2021). The results of Milisavljevic et al. (2014) are consistent with this scenario. The authors observed the spectra of Type Ic supernova

SN 2012ap as a function of time and found that the absorption strength of DIB λ 4430 decreases by a factor of two over a 10-day period, an evidence of the DIB λ 4430 carrier being ionized by the radiation produced by the supernova. This indicates that the DIB λ 4430 carrier tends to be less abundant in environments with strong radiation fields. The authors also found that DIB λ 5780 shows a different trend. Its absorption strength increases by $\sim 20\%$ over a similar timescale of the change of DIB λ 4430. The authors argued that the carrier of DIB λ 5780 might be photo-products of the carrier of DIB λ 4430. In addition, with a relatively lower gas density in the CGM (e.g., Tumlinson et al. 2017), materials in the CGM are expected to be in higher ionization states than gas and molecules in the ISM. Therefore, if the carrier of DIB λ 4430 is neutral or in lower ionization state, it is possible that they are in a higher ionization state in the CGM. This can be another factor for the non-detection of DIB λ 4430 in MgII absorbers.

4. CONCLUSIONS

In this work, we performed a deep search for DIB λ 4430, one of the strongest DIBs observed in the Milky Way, in the extragalactic circumgalactic gas

traced by MgII absorption lines at $0.4 < z < 1.0$. To this end, we obtained high S/N composite spectra using $\sim 60,000$ SDSS absorption line spectra from which we measured the DIB λ 4430 rest equivalent widths. Our results are summarized as follows:

- The composite spectra enable us to probe the DIB λ 4430 rest equivalent widths as a function of MgII rest equivalent widths with absorption strength uncertainty being a few mÅ. However, no DIB λ 4430 absorption signals are detected.
- Adopting the MgII rest equivalent width and dust E(B-V) relation from the literature, we compare the relation between DIB λ 4430 absorption strength and E(B-V) in the CGM and the relation obtained in the ISM of the Milky Way. We find that with the same E(B-V), the DIB λ 4430 absorption is lower than the DIB λ 4430 absorption obtained in the Milky Way, yielding $\sim 5\sigma$ deviation between the DIB λ 4430-E(B-V) relation in the CGM and the relation in the ISM.
- We also produce synthetic spectra by adding DIB absorption lines with strengths, following the MW DIB λ 4430-E(B-V) relation, in the quasar spectra, perform the analysis procedure, and demonstrate that the input signals can be recovered and detected with the dataset.

Our results show that with the same reddening values, the abundance of the DIB λ 4430 carrier in the CGM environment is lower than the abundance of the DIB λ 4430 carrier in the ISM environment, indicating that the environmental factors, such as gas density, radiation field, and transportation of materials from the ISM to the CGM, play a key role in regulating the amount of DIB carriers.

This work also demonstrates that probing the DIBs in different environments provides useful information on understanding the nature of DIB carriers. Ongoing and upcoming spectroscopic surveys will offer rich datasets enabling the explorations of DIBs in different environments with unprecedented precision. For example, the Dark Energy Spectroscopic Instrument (DESI) (Levi et al. 2013; DESI Collaboration et al. 2022) will collect a few million quasar spectra and detect hundred thousands of metal absorbers (e.g., Napolitano et al. 2023), which will increase the number of absorption lines by a factor of 4-5 for a similar study of probing DIBs in the CGM environment. In addition, spatial-resolved spectroscopic observations with integral field units for galaxies can potentially be used to map out the DIB distribution in nearby extragalactic galaxies and explore the properties of galaxies and DIBs (e.g., Monreal-Ibero et al. 2018). Finally, the number of spectra of stars and extragalactic sources from sky surveys, e.g., DESI, SDSS-V (Kollmeier et al. 2017), 4MOST (de Jong et al. 2019),

PFS (Takada et al. 2014), continues to grow. The distributions of DIBs in various ISM environments in the Milky Way can be mapped in greater detail, revealing the underlying mechanisms that regulate the production and destruction of DIB carriers.

C.Y.C and T.W.L are supported by the National Science and Technology Council (MOST 111-2112-M-002-015-MY3, NSTC 113-2112-M-002-028-MY3), the Yushan Fellow Program by the Ministry of Education (MOE) (NTU-110VV007, NTU-111V1007-2, NTU-112V1007-3, NTU-113V1007-4), National Taiwan University research grant (NTU-CC-111L894806, NTU-CC-112L893606, NTU-CC-113L891806, NTU-111L7318, NTU-112L7302). C.Y.C acknowledges the support of the National Science and Technology Council (111-2813-C-002-010-M).

Funding for the Sloan Digital Sky Survey IV has been provided by the Alfred P. Sloan Foundation, the U.S. Department of Energy Office of Science, and the Participating Institutions. SDSS acknowledges support and resources from the Center for High-Performance Computing at the University of Utah. The SDSS web site is www.sdss4.org.

SDSS is managed by the Astrophysical Research Consortium for the Participating Institutions of the SDSS Collaboration including the Brazilian Participation Group, the Carnegie Institution for Science, Carnegie Mellon University, Center for Astrophysics — Harvard & Smithsonian (CfA), the Chilean Participation Group, the French Participation Group, Instituto de Astrofísica de Canarias, The Johns Hopkins University, Kavli Institute for the Physics and Mathematics of the Universe (IPMU) / University of Tokyo, the Korean Participation Group, Lawrence Berkeley National Laboratory, Leibniz Institut für Astrophysik Potsdam (AIP), Max-Planck-Institut für Astronomie (MPIA Heidelberg), Max-Planck-Institut für Astrophysik (MPA Garching), Max-Planck-Institut für Extraterrestrische Physik (MPE), National Astronomical Observatories of China, New Mexico State University, New York University, University of Notre Dame, Observatório Nacional / MCTI, The Ohio State University, Pennsylvania State University, Shanghai Astronomical Observatory, United Kingdom Participation Group, Universidad Nacional Autónoma de México, University of Arizona, University of Colorado Boulder, University of Oxford, University of Portsmouth, University of Utah, University of Virginia, University of Washington, University of Wisconsin, Vanderbilt University, and Yale University.

REFERENCES

- Anand, A., Nelson, D., Kauffmann, G., 2021, *MNRAS*, 504, 65–88
- Bailey, M., van Loon, J., Sarre, P. J., et al. 2015, *MNRAS*, 454, 4
- Baron, D., Poznanski, D., Watson, D. et al. 2015, *MNRAS*, 447, 1, 545–558
- Bordoloi, R., Lilly, S. J., Knobel, C., et al. 2011, *ApJ*, 743, 10. doi:10.1088/0004-637X/743/1/10
- Campbell, E. K., Holz, M., Gerlich, D., et al. 2015, *Nature*, 523, 322
- Campbell, E. K., Holz, M., Maier, J.P., et al. 2016, 822, A17
- Campbell, E. K. Maier, J. P., 2018, *ApJ*, 858, A36
- Cordiner, M. A., Cox, N. L. J., Evans, C. J., et al. 2011, *ApJ*, 726, 39. doi:10.1088/0004-637X/726/1/39
- Cordiner, M. A. 2014, *The Diffuse Interstellar Bands*, 297, 41. doi:10.1017/S174392131301555X
- Cordiner, M. A., Cox, N. L. J., Lallement, R., et al. 2017, *ApJL*, 843, L2
- Cordiner, M. A., Linnartz, H., Cox, N. L. J., et al. 2019, *ApJL*, 875, L28. doi:10.3847/2041-8213/ab14e5
- Cox, N. L. J., Cordiner, M. A., Ehrenfreund, P., et al. 2007, *A&A*, 470, 941–955
- Crawford, M. K., Tielens, A. G. G. M., & Allamandola, L. J. 1985, *ApJ*, 293, L45
- de Jong, R. S., Agertz, O., Berbel, A. A., et al. 2019, *The Messenger*, 175, 3. doi:10.18727/0722-6691/5117
- DESI Collaboration, Abareshi, B., Aguilar, J., et al. 2022, *AJ*, 164, 207. doi:10.3847/1538-3881/ac882b
- Ellison, S. L., York, B. A., Murphy, M. T., et al. 2008, *MNRAS*, 383, 1, 30-34
- Elyajouri, M., Lallement, R., Monreal-Ibero, A., et al. 2017, *A&A*, 600, A129
- Federman, Z., Jackson, S. R., Ng, C., W. M., et al. 2021, *Bulletin of the AAS*, 53(6)
- Fitzpatrick, E. L. & Massa, D. 2007, *ApJ*, 663, 320. doi:10.1086/518158
- Galazutdinov, G. A., Musaev, F. A., Krelowski, J., & Walker, G. A. H. 2000, *PASP*, 112, 648
- Heckman, T. M. & Lehnert, M. D. 2000, *ApJ*, 537, 690. doi:10.1086/309086
- Heger, M. L. 1922, *Lick Obs. Bull.*, 337, 146
- Hobbs, L. M., York, D. G., Snow, T. P. et al. 2008, *ApJ*, 280, 1256
- Hobbs, L. M., York, D. G., Thorburn, J. A. et al. 2009, *ApJ*, 705, 32
- Iglesias-Groth, S. 2007, *ApJL*, 661, L167. doi:10.1086/518832
- Jenniskens, P., Désert, F.-X. 1994, *A&A*, 106, 39
- Junkkarinen, V. T., Cohen, R. D., Beaver, E. A., et al. 2004, *ApJ*, 614, 658. doi:10.1086/423777
- Kollmeier, J. A., Zasowski, G., Rix, H.-W., et al. 2017, arXiv:1711.03234. doi:10.48550/arXiv.1711.03234
- Lai, S.-Y., Witt, A., Alvarez, C., et al. 2020, *MNRAS*, 492, 4, 5853–5864
- Lan, T.-W., Ménard, B., & Zhu, G. 2015, *MNRAS*, 452, 3626
- Lan, T.-W. & Fukugita, M. 2017, *ApJ*, 850, 156. doi:10.3847/1538-4357/aa93eb
- Lan, T.-W., Ménard, B., Baron, D., et al. 2018, *MNRAS*, 477, 3520. doi:10.1093/mnras/sty864
- Lan, T. W. 2020, *ApJ*, 897, 97
- Lawton, B., Churchill, C. W., York, B. A., et al. 2008, *AJ*, 136, 994
- Léger, A. & D’Hendecourt, L., 1985, *A&A*, 146, 81
- Léger, A., D’Hendecourt, L., Verstraete, L. et al. 1988, *A&A*, 203, 145
- Levi, M., Bebek, C., Beers, T., et al. 2013, arXiv:1308.0847
- Linnartz, H., Cami, J., Cordiner, M., et al. 2020, *J. Mol. Spectrosc*, 367, 111243
- Lyke, B. W., Higley, A. N., McLane, J. N., et al. 2020, *ApJS*, 250, 8. doi:10.3847/1538-4365/aba623
- Ménard, B., Nestor, D., Turnshek, D. et al. 2008, *MNRAS*, 385, 2, 1053–1066
- Ménard, B., & Fukugita, M., 2012, *ApJ*, 754, 116
- Merrill, P. W., 1934, *PASP*, 46, 206
- Merrill, P. W., & Wilson, O. C., 1938, *ApJ*, 87, 9
- Milisavljevic, D., Margutti, R., Crabtree, K. N., et al. 2014, *ApJL*, 782, L5. doi:10.1088/2041-8205/782/1/L5
- Monreal-Ibero, A., Weilbacher, P. M., & Wendt, M. 2018, *A&A*, 615, A33. doi:10.1051/0004-6361/201732178
- Napolitano, L., Pandey, A., Myers, A. D., et al. 2023, *AJ*, 166, 99. doi:10.3847/1538-3881/ace62c
- Ng, Y. V., Lan, T.-W., et al. 2025 in prep.
- Priestley, F. D., Chawner, H., Matsuura, M., et al. 2021, *MNRAS*, 500, 2543. doi:10.1093/mnras/staa3445
- Gaia Collaboration, Schultheis, M., H. Zhao, H., T. Zwitter, et al. 2023, *A&A*, 674, A40
- Snow, T. P. 2002, *ApJ*, 567, 407. doi:10.1086/338423
- Snow, T. P., Zukowski, D., Massey, P. 2002, *ApJ*, 578, 877
- Strelnikov, D., Kern, B., & Kappes, M. M. 2015, *A&A*, 584, A55. doi:10.1051/0004-6361/201527234
- Takada, M., Ellis, R. S., Chiba, M., et al. 2014, *PASJ*, 66, R1. doi:10.1093/pasj/pst019
- Tumlinson, J., Peeples, M.S., & Werk, J.K. 2017, *A&A*, 55, 389
- van Loon, J. T., Bailey, M., Tatton, B. L., et al. 2013, *A&A*, 550, A108

- Walker, G. A. H. 1963, MNRAS, 125, 141.
doi:10.1093/mnras/125.2.141
- Webster, A., 1993, MNRAS, 263, 385
- Welty, D. E., Federman, S. R., Gredel, R. et al. 2006, ApJS, 165, 138
- Welty, D. E. 2014, IAU Symposium, 297, 153
- Welty, D. E., Ritchey, A. M., Dahlstrom, J. A., et al. 2014, ApJ, 792, 106. doi:10.1088/0004-637X/792/2/106
- Xiang, F. Y., Li, A., & Zhong, J. X. 2017, ApJ, 835, 107. doi:10.3847/1538-4357/835/1/107
- York, D. G., Adelman, J., Anderson, J. E., et al. 2000, AJ, 120, 1579. doi:10.1086/301513
- York, D. G., Khare, P., Vanden Berk, D., et al. 2006, MNRAS, 367, 945. doi:10.1111/j.1365-2966.2005.10018.x
- York, B. A., Ellison, S. L., Lawton, B., et al. 2006, ApJL, 647, L29. doi:10.1086/505907
- Zhu, G., & Ménard, B. 2013, Ap J, 770, 130
- Zhu, G. & Ménard, B. 2013, ApJ, 773, 16. doi:10.1088/0004-637X/773/1/16
- Zhu, G., Ménard, B., Bizyaev, D., et al. 2014, MNRAS, 439, 3139. doi:10.1093/mnras/stu186
- Zhu, G. 2016, arXiv:1612.06037. doi:10.48550/arXiv.1612.06037